Domain Nucleation Rates and Interfacial Line Tensions in Supported Bilayers of Ternary Mixtures Containing Galactosylceramide

Craig D. Blanchette,*† Wan-Chen Lin,* Christine A. Orme,† Timothy V. Ratto,† and Marjorie L. Longo‡
*Biophysics Graduate Group, College of Biological Sciences, †Biophysical and Interfacial Science Group, Chemistry and Material Science, Lawrence Livermore National Laboratory, Livermore, California; and ‡Department of Chemical Engineering and Materials Science, University of California, Davis, California

ABSTRACT Domains within the plane of the plasma membrane, referred to as membrane rafts, have been a topic of considerable interest in the field of membrane biophysics. Although model membrane systems have been used extensively to study lipid phase behavior as it relates to the existence of rafts, very little work has focused on either the initial stage of lipid domain nucleation, or the relevant physical parameters such as temperature and interfacial line tension which control nucleation. In this work, we utilize a method in which the kinetic process of lipid domain nucleation is imaged by atomic force microscopy and modeled using classical theory of nucleation to map interfacial line tension in ternary lipid mixtures. These mixtures consist of a fluid phase lipid component (1,2-dilauroyl-*sn*-glycero-3-phosphocholine, 1-palmitoyl-2-oleoyl-*sn*-glycero-3-phosphocholine, or 1,2-dioleoyl-*sn*-glycero-3-phosphocholine), a solid phase component (galactosylceramide), and cholesterol. Interfacial line tension measurements of galactosylceramide-rich domains track with our previously measured area/perimeter ratios and height mismatches measured here. Line tension also follows known trends in cholesterol interactions and partitioning, as we observed previously with area/perimeter ratios. Our line tension measurements are discussed in combination with recent line tension measurements to address line tension regulation by cholesterol and the dynamic nature of membrane rafts.

INTRODUCTION

Membranes formed from multiple lipid components can laterally separate into coexisting phases, or domains, with distinct compositions. Theoretical frameworks link domain interfacial line tension (γ) to characteristics that may help us to understand membrane rafts: critical nuclei size (r_c), nucleation rate (J), and when combined with bending parameters, pattern formation (1,2). Measurements of γ were limited to a single ternary membrane composition (1). Baumgart et al. (1) used shape analysis of giant unilamellar vesicles, applicable to low domain bending modulus (L-L) phase coexistence, to demonstrate that γ is of magnitude 1 pN. This method was extended recently by including micropipette aspiration, allowing normal pressures to be varied and a better fit to the data (1,3). The investigators characterized γ-values for five ternary mixtures within the L-L coexistence regime. This more accurate method yielded γ-values that decreased from ~3 pN at 16 mol % cholesterol (chol) to 0.5 pN at 40 mol % chol near the upper (referring to high chol concentration) critical mixing or demixing point. Recently, we applied classical theory of nucleation to domains in two-component supported lipid bilayers to determine γ-values (4). This method, applicable to L-solid (S) and L-L phase coexistence, gave a line tension of ~4 pN for high domain bending modulus (L-S) phase coexistence where DSPC-rich domains in the two leaflets were in registry (symmetric). The value was ~2 pN for galactosylceramide (GalCer)-rich domains residing in one leaflet (asymmetric), i.e., one-half of the symmetric value in proportion to the relative hydrophobic mismatch.

In two related studies, we compared the microstructure and phase behavior of three ternary mixtures at varying chol concentrations (5,6). Each of these mixtures contained GalCer, chol, and a different fluid phase phosphatidylcholine (PC) that varied in level of unsaturation. Thus, we systematically varied the fluid phase lipid component to modulate the strength of the chol-fluid phase PC interaction (1,2-dilauroyl-*sn*-glycero-3-phosphocholine (DLPC) > 1-palmitoyl-2-oleoyl-*sn*-glycero-3-phosphocholine (POPC) > 1,2-dioleoyl-*sn*-glycero-3-phosphocholine (DOPC)) according to the literature (7–13). GalCer, a glycosphingolipid, was chosen as the domain species for these studies because it is believed to be a major raft component in epithelial cell plasma membranes, where GalCer may be a target of the HIV virus in sexual transmission and in impairment of cell function (14–16). We found that GalCer domain microstructure and phase were affected by the interaction strength between fluid-phase lipid and chol and also by related partition behavior of chol. Our findings pointed to a complex interplay between acyl-chain unsaturation, hydrophobic mismatch, and sterol concentration controlling γ, and thus microstructure and dynamics in multicomponent lipid systems, such as cell membranes.

Here we map γ with chol concentration for the three ternary lipid mixtures (fluid phase PC/GalCer/chol) that vary in acyl-chain unsaturation of the fluid-phase PC. We compare our results with area/perimeter (A/P) ratios previously

Submitted September 26, 2007, and accepted for publication November 28, 2007.

Address reprint requests to Marjorie L. Longo, Tel.: 530-754-6348; E-mail: mllongo@ucdavis.edu.

Editor: Lukas K. Tamm.

0006-3495/08/04/2691/07 $2.00

doi: 10.1529/biophysj.107.122572

measured and height mismatches measured here. As with the binary mixture γ-values measured by us earlier, domain nucleation and growth in these ternary systems were imaged by atomic force microscopy (AFM) at various undercoolings. The faster J-values in the presence of chol required the use of growth curves to estimate more accurately nucleation events and therefore the time span of the nucleation phase. Classical theory of nucleation is applied to these J measurements to yield γ-values. This nucleation method is not limited to domains of low bending modulus and therefore, chol concentration was varied from 0 mol % to 18 mol % spanning the high domain bending modulus (L-S) regime and low domain bending modulus (L-L) regime. Our γ measurement at 15 mol % chol agrees well with the measurement by Baumgart and co-workers using GUVs and most of the remaining line tensions were measured at chol concentrations unavailable to any other method, i.e., the transitional region from L-L to L-S coexistence. Uncertainties in estimation of transitional enthalpies prevent γ measurements at higher chol concentrations by this nucleation method. We relate our results to those of Baumgart and co-workers and the regulation of line tension and phase by chol, chain unsaturation, and hydrophobic mismatch in biological membranes. We also comment on the role of nucleation and growth rate on domain size and shape in model membranes.

MATERIAL AND METHODS

Materials

GalCer (cerebrosides, a mixture of nonhydroxylated and hydroxylated GalCer with tail lengths varying from 16 to 24 carbons) was purchased from Matreya (Pleasant Gap, PA; see Matreya handbook for exact percentage of each tail length). DOPC, POPC, DLPC, and cholesterol were purchased from Avanti Lipids (Alabaster, AL). All materials were used without further purification. All water used in these experiments was purified in a Barnstead Nanopure System (Barnstead Thermolyne, Dubuque, IA) with a resistivity $\geq$17.9 MΩ and pH 5.5.

SLB preparation

Supported lipid bilayers were formed using the vesicle fusion method, which has been described elsewhere (4–6,17–19). Samples containing 0 mol % chol consisted of 60 mol % of fluid-phase PCs (DLPC, POPC, or DOPC) and 40 mol % GalCer. As chol was added to the lipid mixture, the mol % of fluid lipid and GalCer were equivalently decreased (e.g., at 10 mol % chol, there was 55 mol % fluid and 35 mol % GalCer). Lipid mixtures containing the appropriate mole ratio in chloroform were dried in a clean glass reaction vial under a slow stream of N_2. The dried lipid film was resuspended with nanopure water to a final lipid concentration of 0.5 mg/ml. The lipid suspension was incubated in a 70°C water bath for 5 min followed by a 15-s vortexing period. The lipid suspension, consisting of giant multilamellar vesicles, was transferred to a plastic tube at room temperature before further treatment. A suspension of small unilamellar vesicles (SUVs) was formed by sonicating the giant multilamellar vesicle suspension with a tip sonicator (Branson Sonifier, model 250; Branson Ultrasonics, Danbury, CT) at the highest power until the suspension reached clarity. The suspension of SUVs was then allowed a 30-min time period to cool to room temperature. A 500-μl aliquot of the SUV suspension was deposited onto freshly cleaved room-temperature mica contained within the closed fluid cell. The vesicle droplet was allowed to incubate on the mica disk for 30 min and then rinsed 40 times with 500-μl aliquots of purified water to remove excess vesicles.

AFM imaging

Samples were imaged with an Asylum MFP-3D Stand Alone Atomic Force Microscope (Asylum Research, Santa Barbara, CA) in contact mode. Sharpened, coated AFM microlevers (Model MSCT-AUHW, Veeco, Woodbury, NY) with nominal spring constants between 0.01 and 0.05 N/m were used for all scans. Hydration of the samples during scanning was maintained using a closed fluid cell (Asylum Research) and the BioHeater (Asylum Research) was used for temperature control. To capture GalCer-rich domain nucleation and growth at undercooled conditions, scan rates ranged from 20 to 40 s/image depending on the scan size. Due to the rapid scan rates, AFM images were of lower resolution, but the deflection image was sufficient to analyze GalCer-rich domain growth.

RESULTS AND DISCUSSION

Classical theory of nucleation (CNT)

Lipid domain nucleation is analogous to a two-dimensional fluid where one component is crystallizing from the melt. According to classical nucleation theory (CNT) there exists an activation barrier to nucleation, ΔG^*, which depends on the interfacial line tension between the crystallizing phase and the surrounding medium, $\Delta G^* = \pi\gamma^2 a_g T_{trans}/\Delta H \Delta T$. Where a_g is the molar area of the crystallizing molecules, ΔT is the degree of undercooling ($T_{trans} - T$), T_{trans} is the measured liquidus or miscibility temperature for L-S and L-L phase coexistence, respectively; ΔH is the enthalpy of the crystallizing phase, and γ is the interfacial line tension. CNT defines the nucleation rate, J, using an Arrhenius-type expression,

$$J = A\exp\left(\frac{-\Delta G^*}{kT}\right) = A\exp\left(\frac{-\pi\gamma^2 a_g T_{trans}}{kT\Delta H\Delta T}\right), \qquad (1)$$

where k is the Boltzmann constant and A is a preexponential factor. Equation 1 was derived for a two-dimensional domain geometry (a three-dimensional derivation can be found in (20)). To apply CNT to calculate γ-values for phase-separating GalCer-rich domains, it was necessary to undercool supported lipid bilayers to various points below T_{trans} (ΔT) and measure J-values as a function of $1/T\Delta T$. This was done for supported lipid bilayers consisting of the following ternary mixtures: DLPC/GalCer/chol, POPC/GalCer/chol, and DOPC/GalCer/chol. In these ternary mixtures GalCer-rich domains are asymmetric and exist exclusively in the leaflet distal to the substrate, possibly reflecting an asymmetric distribution in vesicles used to make the supported bilayers (5,6). The composition of the distal leaflet appears to be similar to the lipid composition used to make the supported bilayer, as documented previously (5).

Measuring nucleation rates

Measurements of J were taken as a function of undercooling or $\Delta T = T_{trans} - T$. The T_{trans} of the lipid mixture was de-

termined by initially heating the bilayer to 55°C for 30 min to ensure homogeneous mixing. The temperature was then decreased (0.1°C/min) until GalCer-rich domain nucleation was observed, followed by slowly heating (0.1°C/min) until GalCer-rich domains were no longer observed. The T_{trans} was calculated by averaging these two temperatures. To ensure the accuracy of T_{trans} within ± 0.25°C, the bilayer was quenched to 0.25°C above the calculated T_{trans} and imaged for 10–20 min to ensure GalCer-rich domain nucleation was not observed. It is worth noting that there was an observed decrease in T_{trans} at increased chol mol % for ternary mixtures containing DOPC and POPC. This was an expected compositional effect resulting from both decreased GalCer/DOPC ratio and increased chol mol %. Above 10 mol % chol this effect was shown to be more dramatic for POPC than DOPC, where the temperature of nucleation was suppressed to lower temperatures than that of DOPC (~3°C). As a result nucleation occurred at temperatures slightly too low to conduct undercooled nucleation experiments, therefore 10 mol % chol was the highest concentration where J could accurately be measured for ternary mixtures containing POPC. Bilayers were then heated to 5°C above the T_{trans} for 30 min and then rapidly quenching (~6–10°C/min) to various temperatures below the T_{trans} (ΔT). The bilayer was imaged throughout the process to ensure nucleation did not occur until the desired temperature was reached.

For each ΔT, small GalCer-rich domains (<500 nm, Fig. 1, *open circles*) appeared during the course of the first scan, which could have only nucleated in the previous seconds based upon a scan rate of 20–40 s per frame. As the scan proceeded, a variation in GalCer-rich domain size was observed as expected for domains that had nucleated at different times and were growing. Under these conditions, the time of nucleation for all GalCer-rich domains could not be determined from the image alone. Since J represents the number of nuclei divided by the AFM scan area and the time period of nucleation it was necessary to determine the time each domain nucleated relative to each other to calculate J. To adjust for this, domain growth was monitored for the domains that initially appeared smallest. This data was used to establish growth curves. From these curves it was determined that after the domain area was normalized (where A_N is area (A) normalized by the final area (A_f), i.e., (A/A_f)), for a given bilayer composition, domain growth curves followed strikingly similar growth patterns (i.e., the growth curves strongly overlapped) (Fig. 2). In addition it was determined that the growth curves fit well to $A_N = 1 - B \times \exp(-kt^n)$, where B, k, and n are constants (Fig. 2, *solid lines*). This expression derives from the Kolmogorov-Johnson-Mehl-Avrami model that has been used by us recently to evaluate kinetic parameters of growth in binary supported lipid bilayers (21). By using the normalized domain area for domains that had already entered the growth phase during the initial scan, the time of nucleation for each domain (i.e., when $A_N = 0$) was readily back-calculated through the fit equation. The nucleation rate, J, is the number of nuclei that form per unit area per unit time. It was measured by taking the number of nucleation events that occurred divided by the AFM scan area and the time period between the first and last observed nucleation events. This method was used to calculate J-values at all lipid compositions and $1/T\Delta T$ (examples in Fig. 3, *A–C*). This data was fit to Eq. 1 and the fit was used to calculate γ-values (discussed below, fits are shown in Fig. 3, *solid lines*). Nucleation occurred randomly upon sequential thermal quenches (example in Fig. 4), an indication of homogeneous nucleation, a necessary requirement for application of Eq. 1. After growth at ΔT was complete, GalCer-rich domain density and size in the monitored region was not noticeably different from other regions in the same sample, indicating that tip-sample interactions did not alter nucleation or growth.

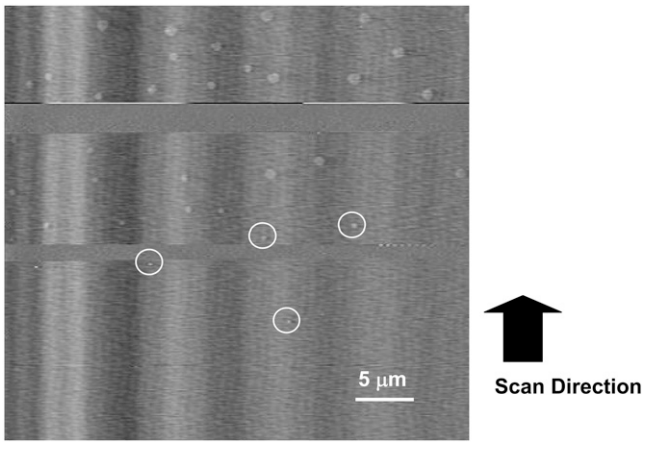

FIGURE 1 Nucleation and growth of GalCer-rich domains occur within the same scan. AFM image of the first scan of a POPC/GalCer/chol mixture containing 7.5 mol % chol quenched to 39°C ($\Delta T = 2.5$°C). Open circles denote first nucleation observed.

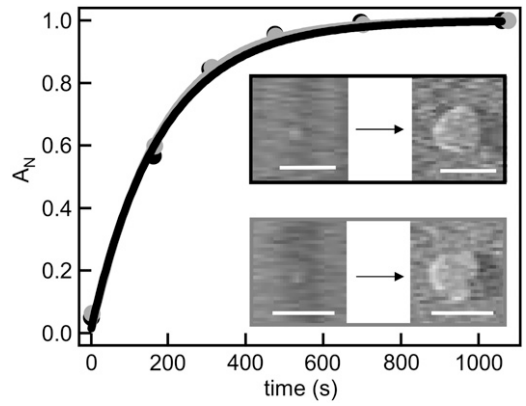

FIGURE 2 Normalized growth curves for two separate GalCer-rich domains in a bilayer of DLPC/GalCer/chol containing 5.0 mol % chol ($\Delta T = 2.5$°C). (*Inset*) Images of initial nucleation and growth of the domains shown in graph. Solid outlined images represent the solid growth curve and shaded outlined images represent shaded growth curves. Scale bars 5 μm.

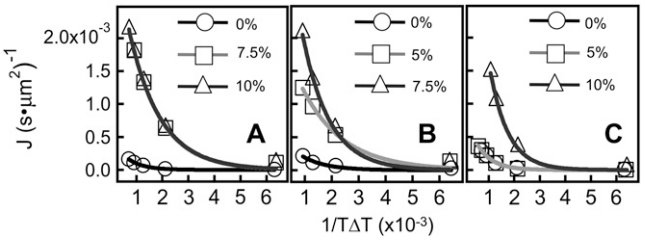

FIGURE 3 Nucleation rates as a function of $1/T\Delta T$ for DLPC/GalCer (*A*), POPC/GalCer (*B*), and DOPC/GalCer (*C*) mixtures at various chol mole percentage. Mole percentage of chol indicated in graphs. Standard propagation of error analysis (37) was used to ascertain error in measurements. The error in both dimensions was within the same size as data points except at large $1/T\Delta T$ (close to the T_m), where the error is $\sim\pm30\%$ for $1/T\Delta T$.

Calculating interfacial line tensions

Calculating γ-values from the fits to Eq. 1 requires the molar area and enthalpy of the phase transition at all compositions studied. Using monolayers at the air-water interface the molecular area of GalCer has been shown (22) to change by $<6\%$ up to 50 mol % chol (within the error of the experimental data), therefore this parameter was left constant as a function of chol mol % ($a_g = 2.5 \times 10^{17}$ μm^2/mole). Several studies have examined the effects of chol on the enthalpy of phase transitions, particularly in 1,2-dipalmitoyl-*sn*-glycero-3-phosphocholine (23). From this work it has been shown that although chol's effect up to 5–7.5 mol % chol is negligible, ΔH begins to decrease between 10 and 20 mol % with a reported reduction of $\sim$23% at 20 mol % chol (23). Therefore, to account for this effect, the percent reduction in ΔH of GalCer upon addition of chol for the ternary mixtures examined in this study was determined from the published literature (24). The following values were used: (0–7.5 mol % chol, 26,778 J/mole; 10 mol % chol, 23,430 J/mole; 12 mol % chol, 22,172 J/mole; 15 mol % chol, 20,913 J/mole; and 18 mol % chol, 20,646 J/mole).

The implicit assumption in the methods used to determine the enthalpy of the phase transition of GalCer is that chol is evenly distributed throughout the bilayer such that the GalCer-rich domains contain the same mole fraction of chol that was added to the initial vesicle solution. From previous studies where we have examined the phase behavior of GalCer in these ternary mixtures, this assumption appears to be valid for the mixtures containing POPC and DOPC up to and including 10 mol % chol (6). For those mixtures, we observed the solid to liquid transition of GalCer-rich domains at 10 mol % chol, the expected transition for pure GalCer. At 20 mol % chol, for similar DOPC-containing ternary mixtures, Veatch et al. (25) observed no significant enrichment of chol in the more ordered phase. For POPC-containing mixtures above 10 mol % chol, a lowered T_{trans}, prevented us from conducting experiments. As described in a previous publication we observe that in the DLPC mixtures, GalCer-rich domains remain in the solid phase at increasing chol mol % and chol preferentially partitions to the DLPC-rich fluid phase (6). Therefore one would expect the enthalpy of the fluid-solid GalCer transition to be only marginally affected at increasing chol mole fraction. Thus the enthalpy value at 0 mol % chol (26,778 J/mole) was used at all chol mol % in the ternary mixtures containing DLPC.

Using these published ΔH and molar area values, γ was calculated by fitting J as a function of $1/T\Delta T$ to Eq. 1 (*curves* in Fig. 3) for the three ternary mixtures as a function of chol. Thus the method employed in this study has allowed for the quantitative mapping of γ for different ternary lipid mixtures as shown in Fig. 5 *A*. This is possible because ΔH is still significant at these compositions and we assume that it can be used to represent the bulk enthalpy difference between the GalCer-rich domains and surrounding lipids.

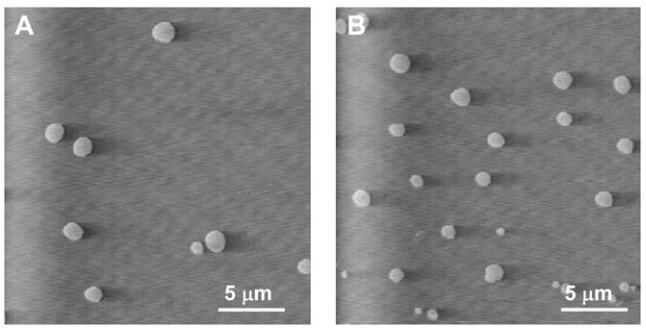

FIGURE 4 Same region of a DLPC/GalCer/chol bilayer containing 10 mol % chol quenched to 40°C ($\Delta T = 1.5$°C) (*A*) and 39°C ($\Delta T = 2.5$°C) (*B*). Sites of domain nucleation were independent of previous thermal quench suggesting homogeneous nucleation.

Area/perimeter ratios, height mismatches, and partitioning behavior

We would expect from CNT that if the domain species concentrations are relatively fixed, fast nucleation rates lead to many small domains whereas slow nucleation rates lead to fewer but larger domain sizes. Indeed, trends in J (Fig. 5 *B*), calculated using our measured γ-values compare inversely to the trends in the A/P ratio of GalCer-rich domains in the same ternary mixtures as a function of chol (Fig. 5 *C*) measured in our previous studies (5,6). There we had cooled the bilayers at a slow temperature ramp (10°C/hour) and thus nucleation and growth should have occurred at uniformly small ΔT; however, we did not know the exact value as we do here. This study shows that γ and the exact thermal conditions of nucleation and growth are crucial to the observed domain structure. This is particularly the case for the early stages of domain formation before coarsening processes can have a significant impact on domain size and shape.

The measured γ-values at 0 mol % chol reflect the relative height mismatches between GalCer-rich domains and surrounding lipid regions as measured by AFM (compare Fig. 5 *A* to Fig. 5 *D*). As stated in our previous work, we believe that $\leq$5 mol % chol acts as a line active agent, capable of straightening

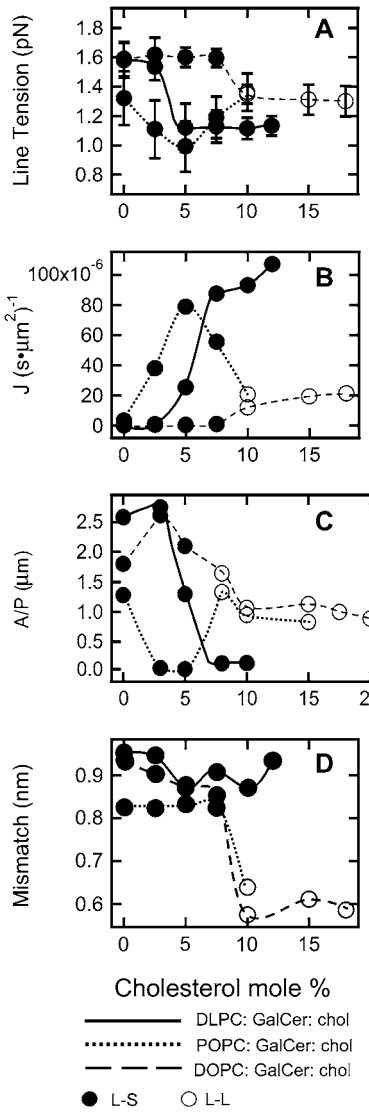

FIGURE 5 (*A*) Line tension (γ) measurements as a function of cholesterol mole percent for GalCer-rich domains. Error bars represent standard deviations from the best fit to Eq. 1. (*B*) Nucleation rates as a function of cholesterol mole percent calculated at $1/T\Delta T = 0.0045$. (*C*) A/P ratios measured at room temperature after slow cooling methods were applied during domain formation as a function of cholesterol mole percent (from Lin et al. (6) with permission). (*D*) Height mismatch measurements taken after domain growth was complete. Standard deviations of height mismatch were all $\sim\pm0.1$ nm.

fluid-phase lipid acyl chains at the narrow (1–2 nm) L-S boundary (5,6). Therefore, reductions in γ at ≤ 5 mol % chol reflect the relative propensity of chol to form liquid-ordered (L_o) phase with species of varying chain unsaturation (DLPC > POPC > DOPC) (7–9). This is a boundary effect and therefore, dramatic changes in height mismatch are not seen in Fig. 5 *D*. Above 5 mol % chol, the γ behavior reflects the partitioning of chol with species of varying chain unsaturation where again DLPC > POPC > DOPC (10). Strong partitioning of chol in the saturated DLPC phase prevents the S→L phase transition (5,6,11,12) of GalCer-rich domains in the DLPC/GalCer/chol mixtures, therefore γ remains lowered, even constant. The constant γ indicates saturation of DLPC by chol at the L-S boundary. Weaker partitioning of chol in the POPC/GalCer/chol and DOPC/GalCer/chol mixtures allows for the S→L phase transition of the GalCer-rich domains (5,6,13) at ~10 mol % chol. Interestingly, these two mixtures have very close γ-values and a similar dramatic drop in height mismatch (compare Fig. 5 *A* to Fig. 5 *D*) at 10 mol % chol. The height mismatches measured at 0 mol % chol and 10 mol % chol are consistent with previous measurements by Le Grimellec and co-workers who studied a POPC/sphingomyelin/chol mixture by AFM (26). In the L-L coexistence region the γ for a single leaflet (1.3 pN at 15 mol % chol) is in good agreement with the measurement by Baumgart and co-workers (3) for two leaflets in registry, 3.3 pN at 16 mol % chol or ~1.5 pN for each leaflet.

Based upon the discussion above, the γ-values at 0 mol % chol and $\geq$10 mol % chol (for DOPC- and POPC-containing mixtures) may be compared to a theoretical model by Chizmadzhev and co-workers predicting monolayer γ from height mismatch and mechanical properties (Eq. 16 in (27)). Since our GalCer-rich domains exist in only one leaflet, comparisons to monolayer γ-values are appropriate. At 0 mol % chol, we use the hydrophobic thickness of GalCer (~2.3 nm (28)), our measured height mismatches, and area compressibility and tilt modulus for monolayers of similar fluid phase lipids (100 mN/m and 40 mN/m, respectively (27)). We obtain by Chizmadzhev's theory ~7.6 pN, ~7.6 pN, and ~5.7 pN for γ of GalCer-rich domains surrounded by DLPC, DOPC, and POPC lipids, respectively. We do the same calculation for 10 mol % chol; however, since the GalCer-rich domain is now fluidized, it should readily deform at the interface and therefore, its mechanical properties should be taken into account. The area compressibility modulus of similar long-chain saturated lipids containing 10–18 mol % chol is approximately double the value for fluid-phase lipids containing no cholesterol (29,30). Doubling the area compressibility modulus and tilt moduli compared to the previous calculation and using the measured thickness mismatch, we obtain ~6.0 pN for γ of GalCer-rich domains surrounded by POPC lipids or DOPC lipids in the presence of 10 mol % chol or 10–18 mol % chol, respectively. Interestingly, although the magnitudes of our measured γ-values are smaller, the percentage differences in γ-values are similar to the predictions. The model by Chizmadzhev and co-workers applies continuum values for the mechanical properties to the domain boundary region that is only several molecules in thickness. Our results suggest that continuum values for mechanical properties are not appropriate, but the general form of the height terms in the model may be correct.

Implications in biological membranes

Combining this work with the results of Baumgart and co-workers (3) it can be implied that γ in ordered lipid domains

in a ternary system is regulated by chol. However, compositional regions exist where γ can be considered steady and overall, γ in domains may vary by less than an order of magnitude, except for the conditions of a critical point. Most noticeably, γ decreases near the L-L to L-S transition as observed by us and toward the upper critical point of the L-L to L transition as observed by Baumgart (3,31). In addition to chol, we found that for L-S coexistence, γ in GalCer-rich domains is regulated by degree of chain unsaturation and height mismatch. Similarly, near the upper critical point, we expect that unsaturation and height mismatch will impact γ as the compositions of the domains and surrounding lipids begin to merge. We would expect that POPC-containing ternary mixtures have lower γ compared to DOPC-containing ternary mixtures similar to our observation in the L-S coexistence regime. POPC, with one unsaturated chain is the more biologically relevant lipid in comparison to DOPC, with two unsaturated chains. Measurements of γ and observations of γ related behavior near the upper critical point of POPC-containing ternary mixtures should be investigated in the future.

In general, mapping γ-values at more compositions may help to reveal the nature of lipid rafts. For example, if cell membranes hover near a phase boundary but not a critical point, the γ of domains may be relatively large ($\sim$1 pN) and domain formation occurs by nucleation and growth whereas near the critical point, low γ results in spinodal decomposition that has been previously observed (32). The larger γ case may be more in line with the experimental evidence that nanoscale ($<$10 nm) rafts in a resting cell are highly unstable structures with lifetimes on the order of nano to microseconds, continuously forming and dispersing such that at any moment there exists a high density of nanoscale raft structures (33–35). According to classical theory of nucleation, the size of a critical or stable nuclei is $r_c = \gamma a_g T_{trans}/\Delta H \Delta T$. Since it is possible that plasma membranes hover near a phase boundary (36), ΔT may be as small as 0.5°C. We show here that γ-values are $\sim$1.3 pN for L-L phase coexistence in GalCer-rich domains contained in one leaflet placing r_c, at $\Delta T \sim 0.5$°C, of $\sim$10 nm. The formation of stable nuclei of $\sim$10 nm will arise infrequently ($\sim 20 \times 10^{-6}\ \mu m^{-2}\ s^{-1}$ as seen in Fig. 5 *B*), supporting the experimental evidence that, in resting cells, rafts are highly unstable and continuously form and dissolve, typical of subcritical nuclei. In addition, experimental evidence indicates that upon external signaling or binding by a pathogen to a lipid or protein component, unstable nanoscale rafts become cross-linked, forming larger, more stable structures (33–35). Some aspect of this process may be related to the phenomena of seeding crystal growth in which nucleation and growth become uncoupled.

C.D.B. acknowledges funding from the Student Employee Graduate Research Fellowship Program of the Lawrence Livermore National Laboratory and National Institutes of Health National Institute of General Medical Sciences (grant No. T32-GM08799). We acknowledge funding by the National Science Foundation Nanoscale Interdisciplinary Research Teams Program (grants No. CHE 0210807 and No. BES 0506602) and the National Science Foundation Materials Research Science and Engineering Centers-Program Center on Polymer Interfaces and Macromolecular Assemblies (National Science Foundation grant No. DMR 0213618). This work was performed under the auspices of the US Department of Energy by the University of California/Lawrence Livermore National Laboratory under contract No. W-7405-Eng-48.

REFERENCES

1. Baumgart, T., S. T. Hess, and W. W. Webb. 2003. Imaging coexisting fluid domains in biomembrane models coupling curvature and line tension. *Nature*. 425:821–824.
2. Omar, W., M. Mohnicke, and J. Ulrich. 2006. Determination of the solid liquid interfacial energy and thereby the critical nucleus size of paracetamol in different solvents. *Cryst. Res. Technol*. 41:337–343.
3. Tian, A., C. Johnson, W. Wang, and T. Baumgart. 2007. Line tension at fluid membrane domain boundaries measured by micropipette aspiration. *Phys. Rev. Lett*. 98:208102.
4. Blanchette, C. D., W.-C. Lin, C. A. Orme, T. V. Ratto, and M. L. Longo. 2007. Using nucleation rates to determine the interfacial line tension of symmetric and asymmetric lipid bilayer domains. *Langmuir*. 23:5875–5877.
5. Blanchette, C. D., W. C. Lin, T. V. Ratto, and M. L. Longo. 2006. Galactosylceramide domain microstructure: impact of cholesterol and nucleation/growth conditions. *Biophys. J*. 90:4466–4478.
6. Lin, W.-C., C. D. Blanchette, and M. L. Longo. 2007. Fluid-phase chain unsaturation controlling domain microstructure and phase in ternary lipid bilayers containing GalCer and cholesterol. *Biophys. J*. 92:2831–2841.
7. de Almeida, R. F. M., A. Fedorov, and M. Prieto. 2003. Sphingomyelin/phosphatidylcholine/cholesterol phase diagram: boundaries and composition of lipid rafts. *Biophys. J*. 85:2406–2416.
8. Lentz, B. R., Y. Barenholz, and T. E. Thompson. 1976. Fluorescence depolarization studies of phase transitions and fluidity in phospholipid bilayers. 2. Two-component phosphatidylcholine liposomes. *Biochemistry*. 15:4529–4537.
9. Vist, M. R., and J. H. Davis. 1990. Phase equilibria of cholesterol/dipalmitoylphosphatidylcholine mixtures: deuterium nuclear magnetic resonance and differential scanning calorimetry. *Biochemistry*. 29:451–464.
10. Lund-Katz, S., H. M. Laboda, L. R. McLean, and M. C. Phillips. 1988. Influence of molecular packing and phospholipid type on rates of cholesterol exchange. *Biochemistry*. 27:3416–3423.
11. Feigenson, G. W., and J. T. Buboltz. 2001. Ternary phase diagram of dipalmitoyl-PC/dilauroyl-PC/cholesterol: nanoscopic domain formation driven by cholesterol. *Biophys. J*. 80:2775–2788.
12. Korlach, J., P. Schwille, W. W. Webb, and G. W. Feigenson. 1999. Characterization of lipid bilayer phases by confocal microscopy and fluorescence correlation spectroscopy. *Proc. Natl. Acad. Sci. USA*. 96:8461–8466.
13. Veatch, S. L., and S. L. Keller. 2002. Organization in lipid membranes containing cholesterol. *Phys. Rev. Lett*. 89:268101.
14. Conboy, J. C., K. D. McReynolds, J. Gervay-Hague, and S. S. Saavedra. 2002. Quantitative measurements of recombinant HIV surface glycoprotein 120 binding to several glycosphingolipids expressed in planar supported lipid bilayers. *J. Am. Chem. Soc*. 124:968–977.
15. Fantini, J., D. G. Cook, N. Nathanson, S. L. Spitalnik, and F. Gonzalez-Scarano. 1993. Infection of colonic epithelial cell lines by type 1 human immunodeficiency virus is associated with cell surface expression of galactosylceramide, a potential alternative gp120 receptor. *Proc. Natl. Acad. Sci. USA*. 90:2700–2704.
16. Maresca, M., R. Mahfoud, N. Garmy, D. P. Kotler, J. Fantini, and F. Clayton. 2003. The virotoxin model of HIV-1 enteropathy: involvement of GPR15/Bob and galactosylceramide in the cytopathic effects

induced by HIV-1 gp120 in the HT-29–D4 intestinal cell line. *J. Biomed. Sci.* 10:156–166.

17. Lin, W. C., C. D. Blanchette, T. V. Ratto, and M. L. Longo. 2006. Lipid asymmetry in DLPC/DSPC-supported lipid bilayers: a combined AFM and fluorescence microscopy study. *Biophys. J.* 90:228–237.
18. Ratto, T. V., and M. L. Longo. 2002. Obstructed diffusion in phase-separated supported lipid bilayers: a combined atomic force microscopy and fluorescence recovery after photobleaching approach. *Biophys. J.* 83:3380–3392.
19. Ratto, T. V., and M. L. Longo. 2003. Anomalous subdiffusion in heterogeneous lipid bilayers. *Langmuir.* 19:1788–1793.
20. Oxtoby, D. W. 1992. Homogeneous nucleation: theory and experiment. *J. Phys. Condens. Matter.* 4:7627–7650.
21. Blanchette, C. D., C. A. Orme, T. V. Ratto, and M. L. Longo. 2007. Quantifying growth of symmetric and asymmetric lipid bilayer domains. *Langmuir.* In press.
22. Ali, S., J. M. Smaby, H. L. Brockman, and R. E. Brown. 1994. Cholesterols interfacial interactions with galactosylceramides. *Biochemistry.* 33:2900–2906.
23. Huang, T. H., C. W. B. Lee, S. K. Dasgupta, A. Blume, and R. G. Griffin. 1993. A C-13 and H-2 nuclear-magnetic-resonance study of phosphatidylcholine cholesterol interactions—characterization of liquid-gel phases. *Biochemistry.* 32:13277–13287.
24. Curatolo, W., and F. B. Jungalwala. 1985. Phase-behavior of galactocerebrosides from bovine brain. *Biochemistry.* 24:6608–6613.
25. Veatch, S. L., I. V. Polozov, K. Gawrisch, and S. L. Keller. 2004. Liquid domains in vesicles investigated by NMR and fluorescence microscopy. *Biophys. J.* 86:2910–2922.
26. Milhiet, P. E., M.-C. Giocondi, and C. Le Grimellec. 2002. Cholesterol is not crucial for the existence of microdomains in kidney brush-border membrane models. *J. Biol. Chem.* 277:875–878.
27. Akimov, S. A., P. I. Kuzmin, J. Zimmerberg, F. S. Cohen, and Y. A. Chizmadzhev. 2004. An elastic theory for line tension at a boundary separating two lipid monolayer regions of different thickness. *J. Electroanal. Chem.* 564:13–18.
28. Kulkarni, K., D. S. Snyder, and T. J. Mcintosh. 1999. Adhesion between cerebroside bilayers. *Biochemistry.* 38:15264–15271.
29. Tierney, K. J., D. E. Block, and M. L. Longo. 2005. Elasticity and phase behavior of DPPC membrane modulated by cholesterol, ergosterol, and ethanol. *Biophys. J.* 89:2481–2493.
30. Needham, D., T. J. Mcintosh, and E. Evans. 1988. Thermomechanical and transition properties of dimyristoylphosphatidylcholine cholesterol bilayers. *Biochemistry.* 27:4668–4673.
31. Esposito, C., A. Tian, S. Melamed, C. Johnson, S.-Y. Tee, and T. Baumgart. 2007. Flicker spectroscopy of thermal lipid bilayer domain boundary fluctuations. *Biophys. J.* 93:3169–3181.
32. Veatch, S. L., and S. L. Keller. 2005. Seeing spots: complex phase behavior in simple membranes. *Biochim. Biophys. Acta Mol. Cell Res.* 1746:172–185.
33. Mayor, S., and M. Rao. 2004. Rafts: scale-dependent, active lipid organization at the cell surface. *Traffic.* 5:231–240.
34. Sharma, P., R. Varma, R. C. Sarasij, I. K. Gousset, G. Krishnamoorthy, M. Rao, and S. Mayor. 2004. Nanoscale organization of multiple GPI-anchored proteins in living cell membranes. *Cell.* 116:577–589.
35. Subczynski, W. K., and A. Kusumi. 2003. Dynamics of raft molecules in the cell and artificial membranes: approaches by pulse EPR spin labeling and single molecule optical microscopy. *Biochim. Biophys. Acta Biomembr.* 1610:231–243.
36. Veatch, S. L. Liquid immiscibility in model bilayer lipid membranes. PhD thesis. University of Washington, Seattle, WA.
37. Taylor, J. R. 1997. Introduction to Error Analysis. University Science Books, Sausalito, CA.